AIMS Mathematics, 10(11): 27217–27234.
DOI: 10.3934/math.20251196
Received: 23 September 2025
Revised: 25 October 2025
Accepted: 12 November 2025
Published: 21 November 2025

https://www.aimspress.com/journal/Math

Research article

Exact analytical solutions of the (2+1)-dimensional Sawada-Kotera equation: A study employing the bilinear neural network method

Zhiyuan Ma[1], Yuanlin Liu[1,2], Zhimin Ma[1,*] and Zhao Li[3]

[1] The Engineering and Technical College of Chengdu University of Technology, Leshan, China

[2] Jiamusi University, Jiamusi, China

[3] College of Computer Science, Chengdu University, Chengdu, China

* **Correspondence:** Email: mazhimin9162@163.com.

Abstract: The (2+1)-dimensional Sawada-Kotera equation is closely related to nonlinear wave applications in higher-dimensional spaces. In this study, we introduce, for the first time, the application of the bilinear neural network method (BNNM) to derive exact analytical solutions for this important equation. Moving beyond traditional approaches, this method allows us to systematically construct a rich family of solutions by designing specific neural network architectures. Specifically, we build single-layer bilinear neural network models to successfully obtain a variety of localized wave solutions. These include lump solutions, which are localized in all directions, breather solutions, which exhibit periodic oscillations in time, and intriguing hybrid lump-soliton solutions. To further explore the equation's complexity, we designed two distinct network architectures, namely [3-2-2-1] and [3-2-3-1], which effectively yielded novel interaction solutions between different wave types and periodic solutions. The characteristics and dynamic behaviors of all these solutions are then thoroughly investigated through detailed graphical representations, including three-dimensional surface plots, contour maps, and density plots, providing vivid insights into their evolution. The success of this work underscores the power of the BNNM framework. Its key advantage lies in its ability to incorporate and generalize numerous classical test functions used in bilinear theory, thereby demonstrating remarkable universality and potential as a unified method for tackling a broad class of nonlinear evolution equations. Our results not only enrich the solution set of the (2+1)-dimensional SK equation, but also establish BNNM as a promising and innovative tool in the field of mathematical physics.

Keywords: (2+1)-dimensional Sawada-Kotera equation; bilinear neural network method; lump solution; breather solutions; lump-soliton solutions; interaction solutions; periodic solution
Mathematics Subject Classification: 9B62, 33B10, 39A12

1. Introduction

In recent years, with the development of nonlinear science, nonlinear evolution equations (NLEEs) have been widely used in many fields [1–3]. Thus, many researchers have conducted in-depth research on the analytical solutions to solve NLEEs. Among them, the Darboux transformation [4], Bäcklund transformation [5], Hirota bilinear method [6, 7], inverse scattering method [8], and homogeneous balance method [9] are all important solution methods. With the aid of these methods, numerous scholars have achieved remarkable research results [10–13]. However, due to the complexity of nonlinear evolution equations, the solution methods are highly dependent on the structure and physical significance of the equations, and there is no universal unified theory at present.

With the rapid development of symbolic computation, Zhang et al. [14–18] proposed the bilinear neural network method (BNNM), which is a novel method that combines the Hirota bilinear method and the neural network model to obtain the exact analytical solution of the nonlinear systems [19, 20]. The nonlinear characteristic between the activation function and the parameters in the bilinear neural network model makes it more flexible to solve the exact analytical solution of NLEEs. Consequently, BNNM [21–24] has garnered extensive attention from researchers, as it provides a universal framework for obtaining accurate analytical solutions of NLEEs and plays a significant role in advancing nonlinear science.

The (2+1)-dimensional Sawada-Sotera (SK) equation [25] was first proposed by Konopelchenko and Dubrovsky. This equation is an integrable system that characterizes higher-order nonlinear wave dynamics and is applicable to various fields involving complex nonlinear wave propagation, such as two-dimensional quantum gravity gauge fields, conformal field theory, and the Liouville flow conservation equations in nonlinear science. The explicit form of the SK equation is given as follows:

$$u_t = u_{xxxxx} + 5u_x u_{xx} + 5uu_{xxx} + 5u^2 u_x + 5u_{xxy} + 5uu_y + 5u_x \partial_x^{-1} u_y - 5\partial_x^{-1} u_{yy}, \tag{1.1}$$

where $u = u(x, y, t)$ and $(\partial x)^{-n} = (\mathrm{d}/\mathrm{d}x)^{-n}$.

By means of the dependent variable transformation

$$u = 2\frac{\partial^2}{\partial x^2}\left[\ln \xi(x, y, t)\right], \tag{1.2}$$

Equation (1.1) is converted into the following bilinear form:

$$\left(\mathrm{D}x^6 - 5\mathrm{D}y^2 + 5\mathrm{D}y\mathrm{D}x^3 + \mathrm{D}x\mathrm{D}t\right)\xi \cdot \xi = 0. \tag{1.3}$$

The generalized bilinear operator proposed by Ma et al. [26]. can transform Eq (1.3) into

$$\begin{gathered}\xi_{xxxxxx}\xi - 6\xi_{xxxxx}\xi_x + 15\xi_{xxxx}\xi_{xx} - 10\xi_{xxx}^2 + 5\xi\xi_{xxxy} - 5\xi_{xxx}\xi_y - 15\xi_{xxy}\xi_x \\ +15\xi_{xx}\xi_{xy} - 5\xi_{yy}\xi + 5\xi_y^2 + \xi_{xt}\xi - \xi_x\xi_t = 0.\end{gathered} \tag{1.4}$$

The specific definition of the Hirota bilinear operator D is as follows:

$$\begin{gathered}\prod_{i=1}^{3} D_\theta^{n_i}(\xi \cdot \xi) = \left(\frac{\partial}{\partial x_1} - \frac{\partial}{\partial x_2}\right)^{n_1} \times \left(\frac{\partial}{\partial y_1} - \frac{\partial}{\partial y_2}\right)^{n_2} \\ \times \left(\frac{\partial}{\partial t_1} - \frac{\partial}{\partial t_2}\right)^{n_3} \xi(x_1, y_1, t_1)\xi(x_2, y_2, t_2)\Big| \; x_2 = x_1, y_2 = y_1, t_2 = t_1,\end{gathered} \tag{1.5}$$

here, $\theta = \theta(x, y, t)$, and n_1, n_2, and n_3 are nonnegative integers.

Recently, the (2 + 1)-dimensional SK equation has attracted extensive attention from scholars. Huang et al. [27] obtained lump solutions and mixed exponential-algebraic solitary wave solutions for the SK equation through methods such as the bilinear form and truncated Painlevé expansion, thereby enriching the dynamical diversity of higher-dimensional nonlinear wave fields. Li et al. [28] proposed a new parameter constraint method based on N-soliton solutions, and successfully constructed resonant Y-type soliton solutions, as well as novel elastic hybrid solutions involving line waves, breather waves, and higher-order lump waves in Eq (1.1), providing new insights for the study of soliton dynamics in higher-dimensional integrable systems. In [29], rational solutions, bright lump waves, bright-dark lump waves, and three families of bright-dark lump wave solutions for the case $p = 3$ of the (2 + 1)-dimensional p-SK equation were obtained. In [30], the authors obtained new N-soliton solutions, higher-order breather solutions (including three types of first-order breathers), higher-order lump solutions via the long-wave limit, hybrid solutions composed of solitons, breathers, and lumps, as well as similar solutions for the generalized SK equation. In [31–33], many different and novel solutions of Eq (1.1) have been obtained.

Unlike traditional symbolic computation methods, the bilinear neural network method constructs test functions composed of multiple neurons and different hidden layers. These test functions are influenced by the selected activation function, and, after solving, can yield various forms of exact analytical solutions. Therefore, BNNM exhibits a certain degree of universality and flexibility. The rest of this work is organized as follows: In Section 2, the bilinear neural network method is introduced, and its corresponding tensor formula is given. In Scetions 3–5, single-layer bilinear neural network model is constructed to solve the exact analytical solutions of Eq (1.4), and further we analyzed their geometric morphology, physical significance, and dynamical properties through graphical representations. In Section 6, bilinear neural network model of [3-2-2-1] was constructed to obtain interaction solutions for the SK equation. In Section 7, a [3-2-3-1] bilinear neural network model was constructed to obtain periodic solution of Eq (1.4). Finally, the paper is summarized in Section 8.

2. BNNM

The bilinear neural networks method (BNNM) comprises two key components: a Hirota bilinear transformation, and a neural network model. Using BNNM involves the following steps:

- By applying the bilinear transformation, NLEEs are converted to a bilinear equation, as shown in the transition from Eq (1.1) to Eq (1.4).
- The bilinear neural network architecture, as illustrated in Figure 1, consists of an input layer, multiple hidden layers, and an output layer. Each neuron is obtained by a linear combination of all neurons from the previous layer with different or identical activation functions and specific weight coefficients. By employing different activation functions, novel output functions (test functions) can be derived. The corresponding tensor formulation is expressed as follows:

$$\Psi = \sum_{n}^{m} W_{l,u} \Xi_l (\xi_l) + b_i, \tag{2.1}$$

where $W_{l,u}$ represents the weight coefficient, Ξ_l represents the activation function, n and m are

positive integers, l represents the hidden layer containing the $m - n$ layer, and b_i represents the threshold (arbitrary constant).

- After substituting Eq (2.1) into Eq (1.4), we obtain a nonlinear equation involving independent variables, weight coefficients, and thresholds. By extracting the coefficients in front of the independent variables and setting the coefficients of the same power to zero, we can derive an overdetermined nonlinear algebraic system that contains only weight coefficients and thresholds. Solving this system yields multiple sets of coefficient solutions, facilitating the analysis of the relationship between weight coefficients and thresholds.
- Select an appropriate set of coefficient relationships from the solution set and substitute them into Eq (2.1) to obtain the solution expression for Eq (1.4). Then, the exact analytical solution of the original equation is derived through Eq (1.2).
- Finally, 3D plots, density plots, contour maps, and others corresponding to the exact analytical solutions of Eq (1.4) are drawn to facilitate an in-depth exploration of the equation's dynamic characteristics and physical significance.

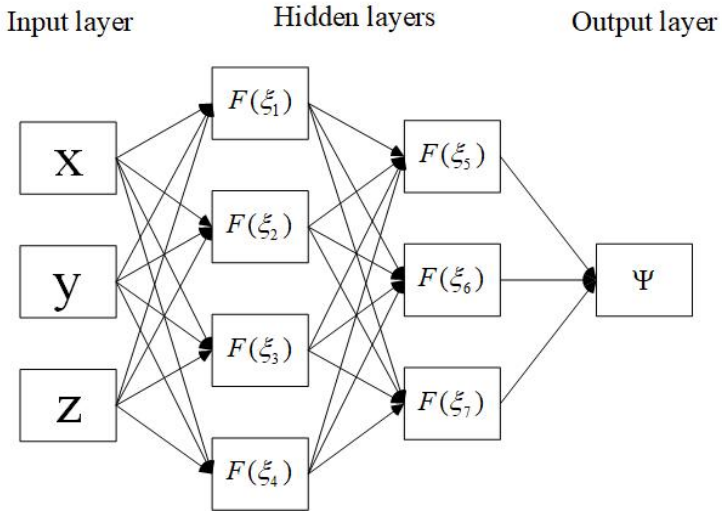

Figure 1. Bilinear neural network model.

The BNNM is a computational approach for solving nonlinear evolution equations by constructing diverse bilinear neural network models. In theory, the depth and the number of neurons in such a model can be continuously increased; however, this not only raises computational costs but may also lead to a phenomenon in which the activation function in the final layer fails to effectively interact with the internal neurons (the weight coefficients in the last layer become zero). This phenomenon results in the inability to obtain the exact analytical solution of Eq (1.4). To prevent performance degradation in the bilinear neural network model, we imposed certain constraints: the first hidden layer contains at most four neurons, the second hidden layer at most three neurons, and $0 < i \leq 7$. These restrictions help ensure model stability when obtaining exact solutions, and prevent degradation caused by the vanishing weight coefficients in the final layer. Exceeding these limits by increasing the number of neurons or network depth not only reduces computational efficiency and prolongs runtime, but also often leads to suboptimal results. These constraints are not universal heuristics for all BNNM, and some equations

may break through this limitation when solving specific exact analytical solutions. The following part is the solution process of various exact analytical solutions for the SK equation.

3. Lump solution

To obtain the lump solution of Eq (1.4), we employ the bilinear neural network model of [3-2-1] for solving, as illustrated in Figure 2a. The specific construction form is as follows:

$$\begin{aligned} \xi_1 &= x \cdot w_{x,1} + y \cdot w_{y,1} + t \cdot w_{t,1} + b_1, \\ \xi_2 &= x \cdot w_{x,2} + y \cdot w_{y,2} + t \cdot w_{t,2} + b_2, \\ \Psi &= w_{1,u} \cdot \xi_1^2 + w_{2,u} \cdot \xi_2^2 + b_3. \end{aligned} \tag{3.1}$$

Substitute Eq (3.1) into Eq (1.4) and collect weight coefficients and thresholds. One set of coefficient solutions is

$$\begin{aligned} b_3 &= \frac{3w_{x,1}^3 w_{1,u}^2 w_{y,1}\left(w_{1,u}w_{y,1}^2 + w_{y,2}^2 w_{2,u}\right)^3}{w_{y,2}^2 w_{2,u}\left(w_{1,u}w_{y,1}^2 - w_{y,2}^2 w_{2,u}\right)^3}, \\ w_{t,1} &= \frac{5w_{1,u}w_{y,1}^2 - 5w_{y,2}^2 w_{2,u}}{w_{1,u}w_{x,1}}, \\ w_{x,2} &= \frac{2w_{x,1}w_{1,u}w_{y,2}w_{y,1}}{w_{1,u}w_{y,1}^2 - w_{y,2}^2 w_{2,u}}. \end{aligned} \tag{3.2}$$

After substituting Eq (3.2) into Eq (3.1),

$$\begin{aligned} \Psi = {} & w_{1,u} \cdot \left(\frac{5t\left(w_{1,u}w_{y,1}^2 - w_{y,2}^2 w_{2,u}\right)}{w_{1,u}w_{x,1}} + x \cdot w_{x,1} + y \cdot w_{y,1} + b_1\right)^2 \\ & + w_{2,u} \cdot \left(\frac{2xw_{x,1}w_{1,u}w_{y,2}w_{y,1}}{w_{1,u}w_{y,1}^2 - w_{y,2}^2 w_{2,u}} + y \cdot w_{y,2} + b_2\right)^2 + \frac{3w_{x,1}^3 w_{1,u}^2 w_{y,1}\left(w_{1,u}w_{y,1}^2 + w_{y,2}^2 w_{2,u}\right)^3}{w_{y,2}^2 w_{2,u}\left(w_{1,u}w_{y,1}^2 - w_{y,2}^2 w_{2,u}\right)^3}. \end{aligned} \tag{3.3}$$

Substitute Eq (3.3) into Eq (1.2). For simplicity in analyzing the dynamics properties of the SK equation, we assign values to the weight coefficients and thresholds as follows:

$$b_1 = b_2 = w_{1,u} = w_{2,u} = w_{y,1} = 1, w_{x,1} = -1, w_{y,2} = -2. \tag{3.4}$$

Finally, we plot the contour map and 3D graph of the lump solution's trajectory. As shown in Figure 2, we observed that while the peak position of the lump solution changes, its shape remains unchanged over time, indicating that its dynamic behavior is stable.

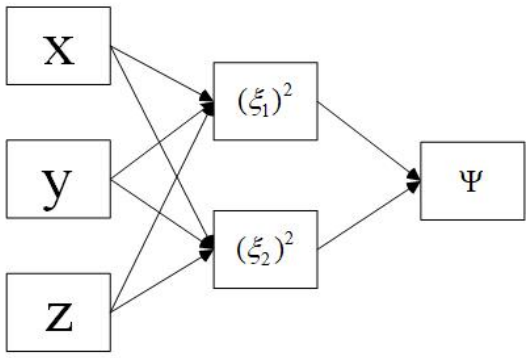

(a)

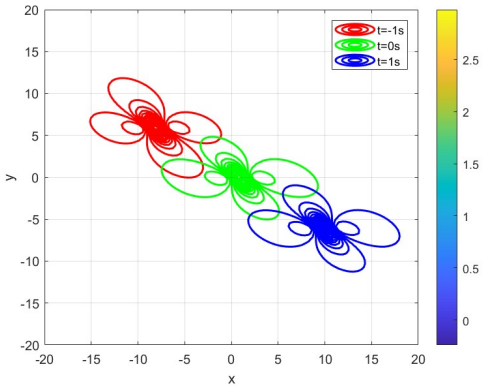

(b)

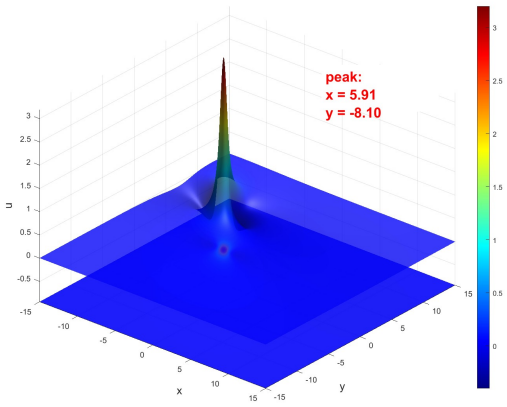

(c) t=-1 s

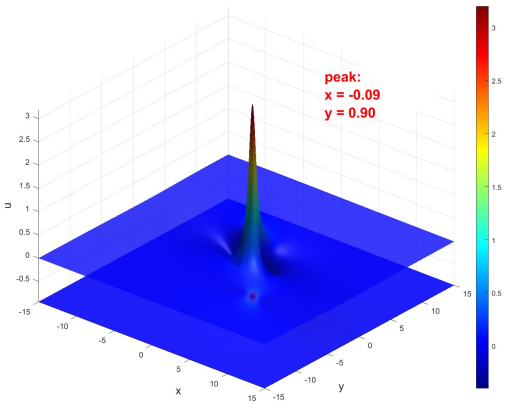

(d) t=0 s

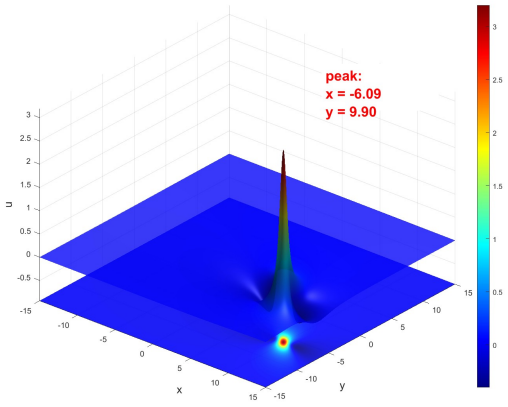

(e) t=1 s

Figure 2. (b) Contour plot showing the trajectory of the lump wave over time, and $(c-e)$ 3D plots of the lump wave at $t \in (-1\text{ s}, 1\text{ s})$.

4. Breather solutions

Breather solutions play an important role in the study of dynamical behaviors in nonlinear systems and are widely found in physical, biological, and engineering systems. We construct a single-layer bilinear neural network model of [3-3-1] to obtain the breather solution of Eq (1.4), as illustrated in Figure 3a. The specific construction is as follows:

$$\begin{aligned} &\xi_1 = t \cdot w_{t,1} + x \cdot w_{x,1} + y \cdot w_{y,1} + b_1, \\ &\xi_2 = t \cdot w_{t,2} + x \cdot w_{x,2} + y \cdot w_{y,2} + b_2, \\ &\Psi = w_{1,u} \cdot \mathrm{e}^{\xi_1} + w_{2,u} \cdot \cos(\xi_2) + w_{3,u} \cdot \mathrm{e}^{-\xi_3} + b_3. \end{aligned} \tag{4.1}$$

In the construction form, the activation function is $\Xi(\xi_1) = \mathrm{e}^{\xi_1}, \Xi(\xi_2) = \cos(\xi_2), \Xi(\xi_3) = \mathrm{e}^{-\xi_3}$. We add the constraint condition $\xi_3 = k \cdot \xi_1$ to facilitate the establishment of a linear relationship between ξ_1 and ξ_3, and k is an arbitrary constant.

Substituting Eq (4.1) into Eq (1.4) yields an overdetermined system of nonlinear algebraic equations. We select an appropriate set of coefficient solutions as follows:

$$\begin{aligned} &k = 1, w_{t,1} = 9w_{x,1}^5 - 90w_{x,1}^3 w_{x,2}^2 + 45w_{x,1} w_{x,2}^4, \\ &w_{t,2} = 45w_{x,2}^4 w_{x,1}^4 - 90w_{x,2}^3 w_{x,1}^2 + 9w_{x,2}^5, \\ &w_{y,1} = -w_{x,1}^3 + 3w_{x,2}^2 w_{x,1}, w_{y,2} = -3w_{x,1}^2 w_{x,2} + w_{x,2}^3. \end{aligned} \tag{4.2}$$

Here, we substitute Eq (4.2) into Eq (4.1):

$$\begin{aligned} \Psi = {} & w_{1,u} \mathrm{e}^{9tw_{x,1}^5 + \left(-90tw_{x,2}^2 - y\right)w_{x,1}^3 + \left(45tw_{x,2}^4 + 3yw_{x,2}^2 + x\right)w_{x,1} + b_1} \\ & + w_{2,u} \cos\left(9tw_{x,2}^5 + \left(-90tw_{x,1}^2 + y\right)w_{x,2}^3 + \left(45tw_{x,1}^4 - 3yw_{x,1}^2 + x\right)w_{x,2} + b_2\right) \\ & + w_{3,u} \mathrm{e}^{-9tw_{x,1}^5 + \left(90tw_{x,2}^2 + y\right)w_{x,1}^3 + \left(-45tw_{x,2}^4 - 3yw_{x,2}^2 - x\right)w_{x,1} - b_1}. \end{aligned} \tag{4.3}$$

For better analysis of its dynamic properties, we assign weight coefficients and thresholds as follows: $b_1 = 1, b_2 = 1, b_3 = 1, w_{1,u} = 1, w_{2,u} = 1, w_{3,u} = 2, w_{x,1} = 1$, and $w_{x,2} = 1$. As shown in Figure 3b, with both the x and y ranges set to $[-10, 10]$, we plot the 3D trajectory of the breather solution for Eq (1.4) along with its density plot at $t = 0s$.

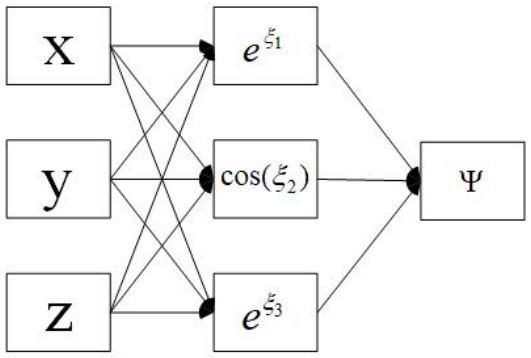

(a)

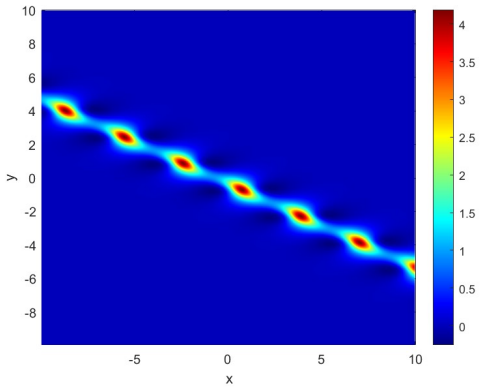

(b)

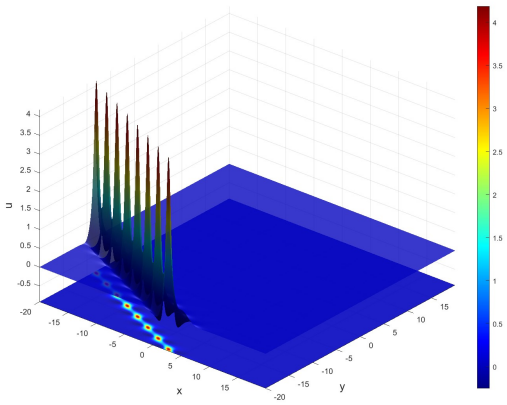

(c) t=-0.5 s

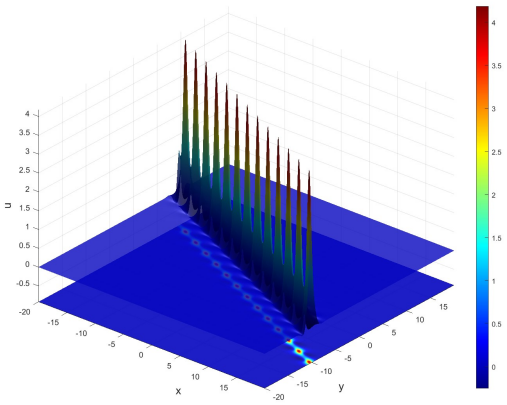

(d) t=0 s

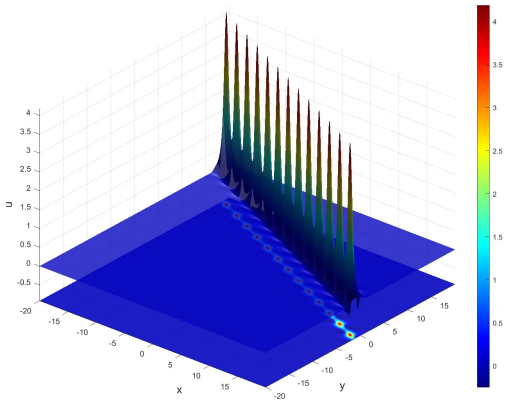

(e) t=0.5 s

Figure 3. (b) Density plot at $t = 0$ s, and (c–e) 3D plots of the breather solution at $t = -0.5$ s, $t = 0$ s, and $t = 0.5$ s, respectively.

As can be observed from Figure (3c) to Figure (3e), the breather solution exhibits spatial localization and self-similarity while maintaining relative stability over time.

5. Lump-soliton solutions

We construct a novel [3-3-1] bilinear neural network model to obtain lump-soliton solutions for the SK equation, as shown in Figure 4a, and the specific form is given by Eq (5.1). By substituting this structure's test function into Eq (1.4), We can obtain a system of nonlinear algebraic equations that contains independent variables, weights w, and biases b_i:

$$\begin{aligned}
\xi_1 &= t \cdot w_{t,1} + x \cdot w_{x,1} + y \cdot w_{y,1} + b_1,\\
\xi_2 &= t \cdot w_{t,2} + x \cdot w_{x,2} + y \cdot w_{y,2} + b_2,\\
\xi_3 &= t \cdot w_{t,3} + x \cdot w_{x,3} + y \cdot w_{y,3} + b_3,\\
\Psi &= w_{1,u} \cdot \xi_1^2 + w_{2,u} \cdot \xi_2^2 + w_{3,u} \cdot \mathrm{e}^{\xi_3} + b_4.
\end{aligned} \tag{5.1}$$

To set the coefficients of different powers of the activation function to zero, one solves this overdetermined nonlinear algebraic system of equations, obtaining a set of coefficient solutions consisting solely of weight coefficients and threshold values. Based on certain physical significance, an appropriate set of coefficient solutions is selected as follows:

$$\begin{aligned}
b_4 &= \frac{4w_{2,u}w_{x,2}^2w_{y,2}}{w_{x,3}^2\left(3w_{x,2}w_{x,3}^2+4w_{y,2}\right)}, w_{y,3} = \frac{w_{x,3}\left(w_{x,2}w_{x,3}^2+2w_{y,2}\right)}{2w_{x,2}},\\
w_{1,u} &= \frac{9w_{x,2}\left(w_{x,2}w_{x,3}^2+\frac{4w_{y,2}}{3}\right)w_{x,3}^2w_{2,u}}{4w_{y,1}^2},\\
w_{t,2} &= \frac{5\left(-9w_{x,2}^2w_{x,3}^4-12w_{x,2}w_{x,3}^2w_{y,2}+4w_{y,2}^2\right)}{4w_{x,2}},\\
w_{t,3} &= -\frac{9w_{x,3}\left(w_{x,2}^2w_{x,3}^4-\frac{20w_{y,2}^2}{9}\right)}{4w_{x,2}^2}, w_{t,1} = \frac{10w_{y,1}w_{y,2}}{w_{x,2}}.
\end{aligned} \tag{5.2}$$

In order to better analyze its dynamic characteristics, we assign Eq (5.2) $b_1 = 1$, $b_2 = 1$, $b_3 = 1$, $w_{2,u} = 1, w_{3,u} = 1, w_{x,2} = 1, w_{x,3} = 1, w_{y,1} = 1$, and $w_{y,2} = 1$ and substitute it back into Eq (1.2). Then, we can obtain the lump-soliton solution of SK equation.

Through 3D plot, the dynamic behavior and characteristics of Eq (1.4) are more intuitively displayed. In Figure 4c to Figure 4f, we can observe the interaction process between lumps and solitons in this equation. Figure 4b shows the contour plot of the motion trajectories of lump-soliton solutions.

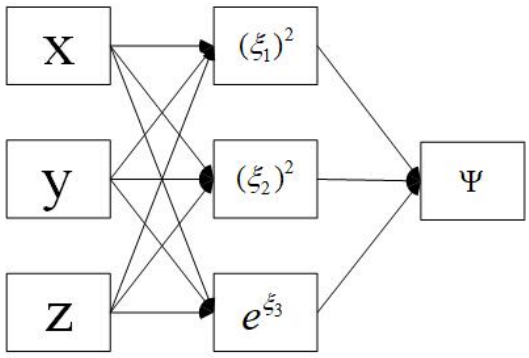

(a)

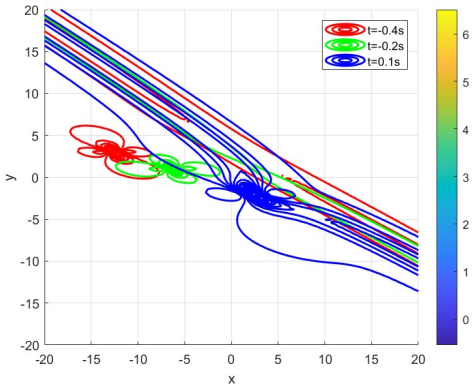

(b)

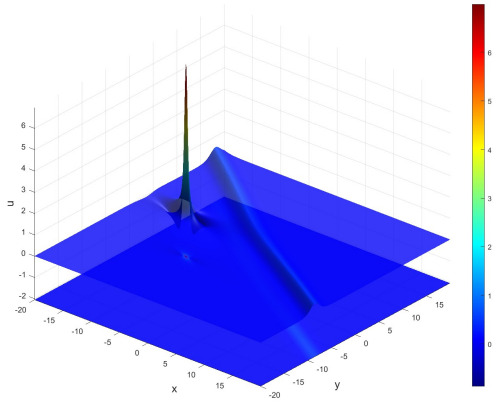

(c) t=-0.4 s

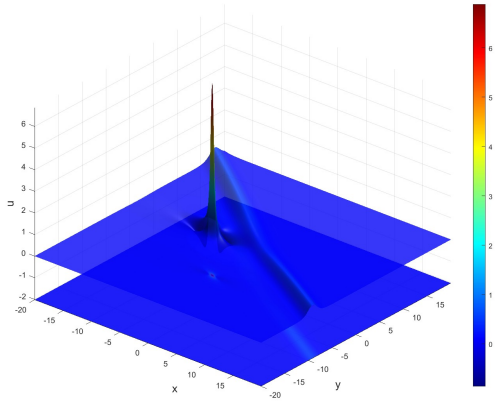

(d) t=-0.2 s

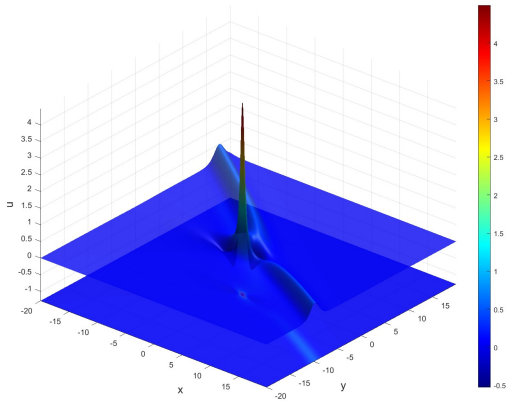

(e) t=0 s

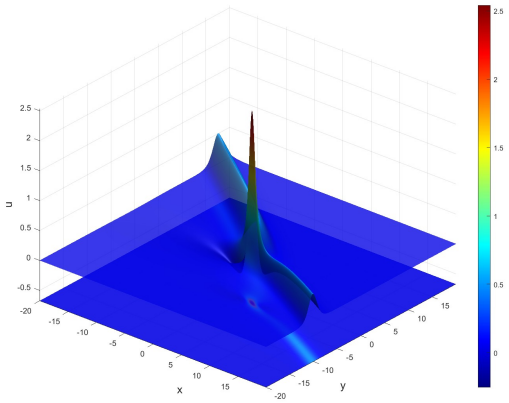

(f) t=0.1 s

Figure 4. (b) Density plot at $t = 0$ s, and (c–e) 3D plots of the breather solution at $t = -0.5$ s, $t = 0$ s, and $t = 0.5$ s, respectively.

6. Interaction solutions

To better analyze the physical significance of Eq (1.4), we constructed a [3-2-2-1] bilinear neural network model with $\Xi(\xi_1) = \xi_1, \Xi(\xi_2) = \mathrm{e}^{\xi_2}, \Xi(\xi_3) = \xi_3^2$, and $\Xi(\xi_4) = \sin(\xi_4)$ as its activation function. As shown in the Figure 5a, the specific tensor formulas are as follows:

$$\begin{aligned}
&\xi_1 = t \cdot w_{t,1} + x \cdot w_{x,1} + y \cdot w_{y,1} + b_1,\\
&\xi_2 = t \cdot w_{t,2} + x \cdot w_{x,2} + y \cdot w_{y,2} + b_2,\\
&\xi_3 = w_{1,3} \cdot \xi_1 + w_{2,3} \cdot e^{\xi_2} + b_3,\\
&\xi_4 = w_{1,4} \cdot \xi_1 + w_{2,4} \cdot e^{\xi_2} + b_4,\\
&\Psi = w_{3,u} \cdot \left(w_{1,3}\xi_1 + w_{2,3}e^{\xi_2} + b_3\right)^2 + w_{4,u} \cdot \sin\left(w_{1,4}\xi_1 + w_{2,4}e^{\xi_2}\right) + b_5.
\end{aligned} \tag{6.1}$$

Substituting Eq (6.1) into Eq (1.4) and collecting the weight coefficients and thresholds, we select one set of suitable coefficient solutions as

$$w_{1,4} = \frac{\sqrt{\frac{w_{y,1}}{w_{x,1}}}}{w_{x,1}}, w_{t,1} = \frac{9w_{y,1}^2}{w_{x,1}}, w_{t,2} = 144w_{x,2}^5, w_{y,2} = -4w_{x,2}^3. \tag{6.2}$$

By substituting Eq (6.2) into Eq (6.1), we can obtain the interaction solution of Eq (1.4).

$$\begin{aligned}
\Psi = {} & w_{3,u} \cdot w_{2,3}^2 \left(\mathrm{e}^{144tw_{x,2}^5 - 4yw_{x,2}^3 + xw_{x,2}}\right)^2\\
& + w_{4,u} \cdot \sin\left(\frac{\sqrt{\frac{w_{y,1}}{w_{x,1}}\left(\frac{9tw_{y,1}^2}{w_{x,1}} + xw_{x,1} + yw_{y,1}\right)}}{w_{x,1}}\right) + b_5.
\end{aligned} \tag{6.3}$$

To briefly analyze its dynamic behavior, we assign the following values to the weight coefficients and thresholds:

$$b_5 = 3, w_{3,u} = 1, w_{4,u} = 1, w_{2,3} = 1, w_{x,1} = 1, w_{x,2} = 0.5, w_{y,1} = 1. \tag{6.4}$$

Substituting Eq (6.4) into Eq (6.3), we can obtain the exact analytical solution of SK equation through the transformation of Eq (1.2).

The domain is defined as $x \in [-20, 20]$ and $y \in [-20, 20]$. Subsequently, density plots of the interaction solutions and 3D graphs of their motion trajectories are plotted. From Figures 5b–5e, it can be observed that these interaction solutions exhibit stability;—over time, they remain parallel and mutually independent, yet their dynamic behaviors remain consistent.

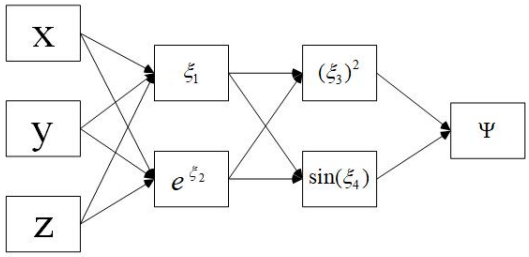

(a)

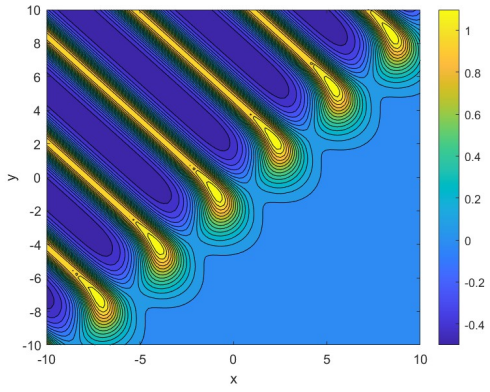

(b)

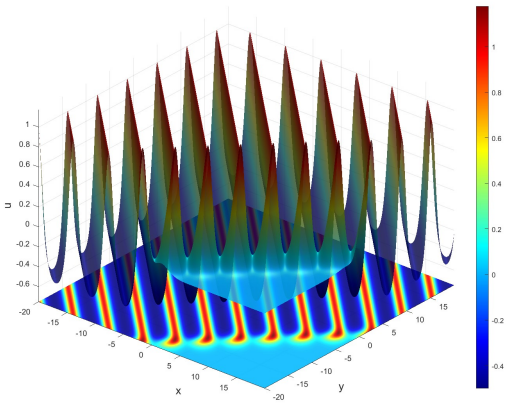

(c) t=-2 s

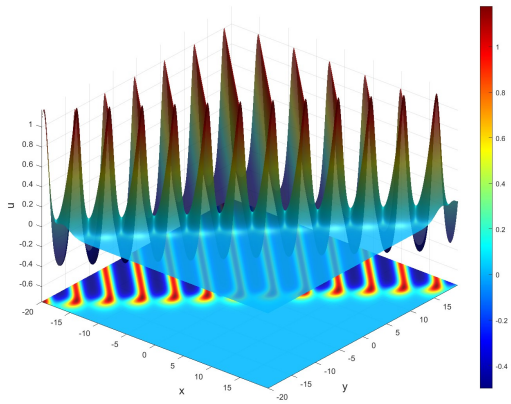

(d) t=0 s

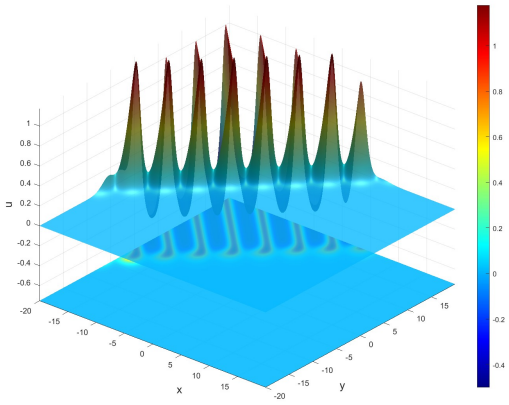

(e) t=2 s

Figure 5. (b) Density plot at $t = 0$ s, and (c–e) 3D plots of the interaction solution at $t = -2$ s, $t = 0$ s, and $t = 2$ s, respectively.

7. Periodic solution

The function ξ in Eq (1.4) is treated as a tensor function within the neural network model. As shown in Figure 6a, a [3-2-3-1] bilinear neural network model is constructed, and its tensor formulation can be expressed as:

$$\begin{aligned}
\xi_1 &= tw_{t,1} + xw_{x,1} + yw_{y,1} + b_1,\\
\xi_2 &= tw_{t,2} + xw_{x,2} + yw_{y,2} + b_2,\\
\xi_3 &= w_{1,3} \cdot \cos(\xi_1) + w_{2,3} \cdot \sin(\xi_2) + b_3,\\
\xi_4 &= w_{1,4} \cdot \cos(\xi_1) + w_{2,4} \cdot \sin(\xi_2) + b_4,\\
\xi_5 &= w_{1,5} \cdot \cos(\xi_1) + w_{2,5} \cdot \sin(\xi_2) + b_5,\\
\psi &= w_{3,u} \cdot \xi_3^2 + w_{4,u} \cdot \xi_4 + w_{5,u} \cdot \sinh(\xi_5) + b_6.
\end{aligned} \tag{7.1}$$

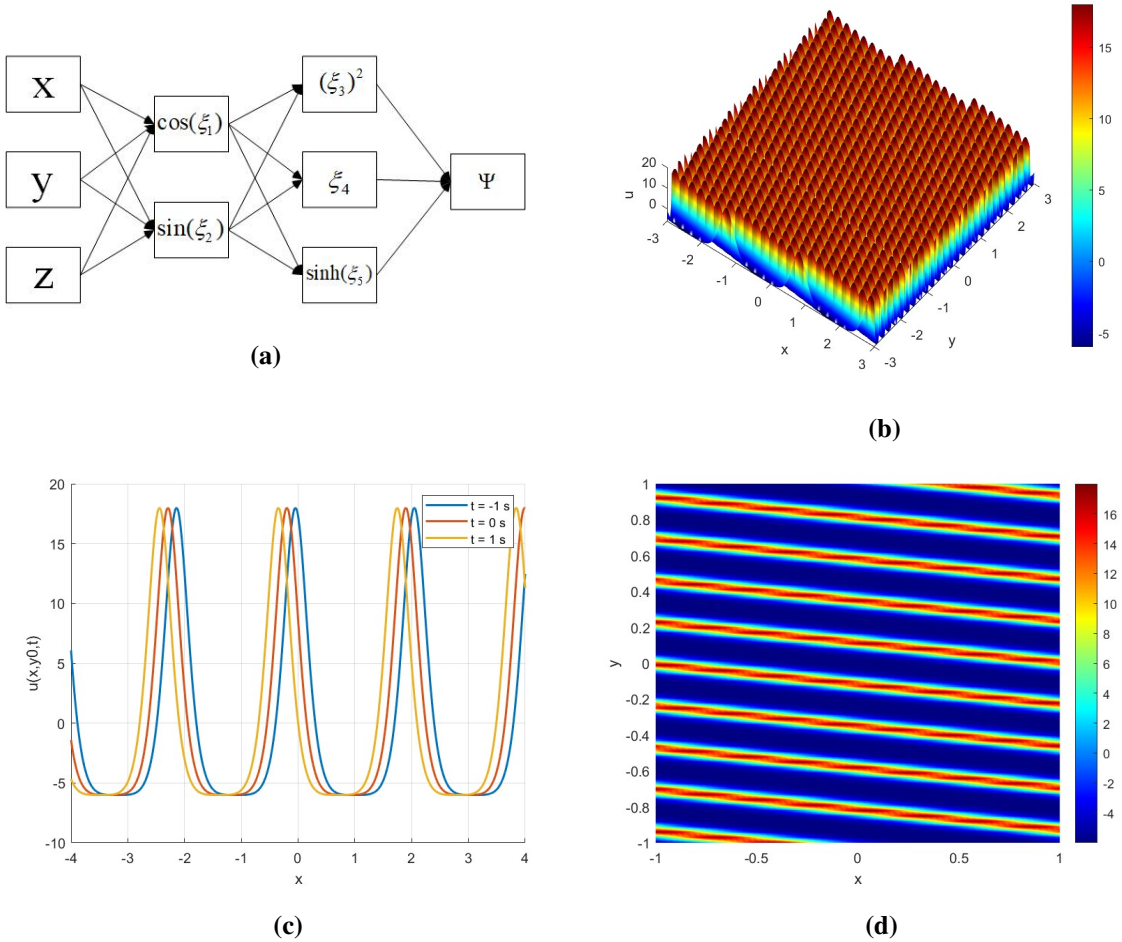

Figure 6. (b) 3D plot of the periodic solution, (c) the x-curve for $t \in (-1\,\text{s}, 1\,\text{s})$, and (d) the density plot.

Here, the activation functions are defined as $\Xi(\xi_1) = \cos(\xi_1), \Xi(\xi_2) = \sin(\xi_2), \Xi(\xi_3) = \xi_3^2, \Xi(\xi_4) = \xi_4$, and $\Xi(\xi_5) = \sinh(\xi_5)$. To prevent degeneration of the bilinear neural network model, we impose the constraint condition $w_{4,u} = w_{5,u}$ during the solution process. During the solving process, when some

of the weight coefficients in the last layer become zero, this type of constraint method is applied to establish relationships between the zero and nonzero weight coefficients, thereby enabling the bilinear neural network model to be successfully used for obtaining the exact analytical solution of Eq (1.1).

By substituting Eq (7.1) into Eq (1.4), we collect the coefficients of the like terms in $x, y, t, \cos(\xi_1), \sin(\xi_2)$, and $\sinh(\xi_5)$. Setting the coefficients corresponding to different powers to zero yields an overdetermined system of nonlinear algebraic equations, one set of which is:

$$\begin{gathered} b_6 = b_6, w_{3,u} = w_{3,u}, w_{4,u} = w_{4,u}, w_{1,4} = w_{1,4}, w_{2,3} = w_{2,3}, \\ w_{2,4} = w_{2,4}, w_{2,5} = w_{2,5}, w_{t,1} = 9w_{x,1}^5, w_{x,1} = w_{x,1}, w_{y,1} = w_{x,1}^3. \end{gathered} \tag{7.2}$$

By substituting Eq (7.2) into Eq (7.1), we can obtain the periodic solution of Eq (1.4). Since the expression of the solution is rather complicated, the parameters of the bilinear neural network model are used instead.

$$\Psi = w_{3,u}w_{2,3}^2 \sin(\xi_2)^2 + \sin(\xi_2) w_{4,u}w_{2,4} + \cos(\xi_1) w_{4,u}w_{1,4} + w_{4,u} \sinh(w_{2,5} \sin(\xi_2)) + b_6. \tag{7.3}$$

To briefly analyze the dynamical properties of the SK equation, we choose the following appropriate values of the parameters:

$$b_6 = 2, w_{3,u} = 1, w_{4,u} = 1, w_{1,4} = 1, w_{2,3} = 1, w_{2,4} = 1, w_{2,5} = 1, w_{x,1} = 3. \tag{7.4}$$

Substituting the assigned Eq (7.4) into Eq (7.3) and then applying the transformation of Eq (1.2), we can finally obtain the exact analytical solution of the SK equation.

Finally, we plot the 3D plot of the periodic solution of Eq (1.4), as shown in Eq (6b), where both x and y range over $[-3, 3]$. To gain a better understanding of its physical properties, Figure 6c presents the x-curve at $y = 2$ within the time interval $[-1s, 1s]$; Figure 6d shows the density plot for x and y ranging over $[-1, 1]$. As an exact analytical solution exhibiting periodic variation over time, the periodic wave solution differs significantly from other types of exact solutions. Unlike localized solutions that are confined to specific regions, it maintains a sustained periodic oscillatory behavior across the entire domain. From Figure 6, it can be observed that this exact analytical solution represents a periodic wave solution that remains stable while propagating over time.

As the framework of the BNNM deepens, the activation functions can be diversified and the number of hidden layers can be increased. However, this also brings a heavy computational burden, making the training time particularly long. When the number of hidden layers and neurons reaches a certain upper limit, the solution often becomes less ideal, and it is easy for some of the weights in the final layer to become zero, which leads to the degeneration of the bilinear neural network model.

In this study, we found that by establishing linear relationships among some of the weights in the final layer, the phenomenon of weights becoming zero can be alleviated, thereby yielding the corresponding exact analytical solutions. Blindly increasing the number of hidden layers and neurons can easily cause overfitting. For example, when using a multilayer bilinear neural network model, the solution obtained may in fact be the similar exact analytical solution that could already be derived by a single-layer bilinear neural network model, resulting in wasted computational cost.

Therefore, the best performance is generally achieved when the number of hidden layers is less than or equal to 2 and the number of neurons is less than or equal to 7. Beyond this range, the effectiveness of bilinear neural network solutions tends to deteriorate.

8. Conclusions

The innovative points of this paper are as follows:

(1) In previous studies, researchers have conducted extensive investigations into exact analytical solutions of the Sawada-Kotera equation, achieving significant results. This paper applies BNNM to the (2+1)-dimensional Sawada-Kotera equation for the first time. We construct multiple single-layer bilinear neural network models to obtain lump solutions, breather solutions, and lump-soliton solutions of the (2+1)-dimensional Sawada-Kotera equation. Furthermore, we draw density plots, contour maps, and 3D plots of their motion trajectories are plotted.

(2) Building upon the single-layer bilinear neural network model, we constructed two bilinear neural network models with structures [3-2-2-1] and [3-2-3-1] to obtain the interaction solutions and periodic solutions of the (2+1)-dimensional Sawada-Kotera equation. We also presented three-dimensional dynamic visualizations and the corresponding density plots of these interaction patterns. By examining the physical phenomena and dynamical behaviors exhibited by these exact analytical solutions, we gained a deeper understanding of the physical significance of the equation, which facilitates the study of nonlinear wave phenomena in the (2+1)-dimensional Sawada-Kotera equation.

(3) In this study, we found that establishing a linear relationship among some final layer weight coefficients can alleviate the phenomenon that this weight coefficient is zero, allowing exact solutions to be obtained. Blindly increasing the number of layers or neurons may also lead to poor performance of bilinear neural network models in solving exact analytical solutions, wasting computational resources. To maintain stability and performance, we constrained the first hidden layer to at most four neurons, the second to at most three neurons, and $0 < i \leq 7$, which helps prevent degeneration while ensuring efficient computation. These constraints are not universal, and some equations may permit exceptions when solving specific exact analytical solutions.

The method of using BNNM to obtain exact analytical solutions of NLEEs has gradually matured and demonstrated considerable generality, thereby advancing the development of nonlinear science. The bilinear residual network method (BRNM) can also, to some extent, alleviate the phenomenon of model degeneration. Currently, most classical frameworks construct the trial functions based on a single hidden layer. Although deeper BNNM architectures allow for more diversified test functions, this comes at the cost of heavier computational burden and significantly prolonged training time, and the effectiveness is often limited with a high risk of overfitting. Future research may overcome this bottleneck by optimizing weight coefficients and activation functions.

Author contributions

Zhiyuan Ma was responsible for writing the original manuscript and applying the methods. Yuanlin Liu and Zhimin Ma were in charge of supervision and formal analysis. Zhao Li was responsible for software.

Use of Generative-AI tools declaration

The authors declare they have used Deepseek in this article. The AI tools were used exclusively for the purpose of language polishing, and improving the fluency and readability of the manuscript.

The AI-assisted improvements are applied throughout the entire text of the manuscript to improve its linguistic quality, and do not affect the core scientific meaning or findings.

Conflict of interest

The authors confirm that they have no conflicts of interest.

References

1. S. Sahoo, S. S. Ray, Lie symmetry analysis and exact solutions of (3+1) dimensional Yu-Toda-Sasa-Fukuyama equation in mathematical physics, *Comput. Math. Appl.*, **73** (2017), 253–260. https://doi.org/10.1016/j.camwa.2016.11.016
2. L. Akinyemi, E. Morazara, Integrability, multi-solitons, breathers, lumps and wave interactions for generalized extended Kadomtsev-Petviashvili equation, *Nonlinear Dyn.*, **111** (2023), 4683–4707. https://doi.org/10.1007/s11071-022-08087-x
3. A. Zafar, M. Shakeel, A. Ali, L. Akinyemi, H. Rezazadeh, Optical solitons of nonlinear complex Ginzburg-Landau equation via two modified expansion schemes, *Opt. Quant. Electron.*, **54** (2022), 5. https://doi.org/10.1007/s11082-021-03393-x
4. X. Zhang, Y. Wang, S. Yang, Soliton solutions, Darboux transformation of the variable coefficient nonlocal Fokas-Lenells equation, *Nonlinear Dyn.*, **112** (2024), 2869–2882. https://doi.org/10.1007/s11071-023-09192-1
5. Y. Wang, X. Lü, Bäcklund transformation and interaction solutions of a generalized Kadomtsev-Petviashvili equation with variable coefficients, *Chinese J. Phys.*, **89** (2024), 37–45. https://doi.org/10.1016/j.cjph.2023.10.046
6. Y. Feng, S. Bilige, Multiple rogue wave solutions of (2+1)-dimensional YTSF equation via Hirota bilinear method, *Wave. Random Complex*, **34** (2024), 94–110. https://doi.org/10.1080/17455030.2021.1900625
7. J. Zhang, J. Manafian, S. Raut, S. Roy, K. H. Mahmoud, A. S. A. Alsubaie, Study of two soliton and shock wave structures by weighted residual method and Hirota bilinear approach, *Nonlinear Dyn.*, **112** (2024), 12375–12391. https://doi.org/10.1007/s11071-024-09706-5
8. I. Toledo, *The direct and inverse scattering problems for the third-order operator*, The University of Texas at Arlington, 2024, Available from: `https://mavmatrix.uta.edu/math_dissertations/163`.
9. X. Wang, Y. Yang, W. Kou, R. Wang, X. Chen, Analytical solution of Balitsky-Kovchegov equation with homogeneous balance method, *Phys. Rev. D*, **103** (2021), 056008. https://doi.org/10.1103/PhysRevD.103.056008
10. T. Alzahrani, M. ur Rahman, Lump, breathing inelastic collision phenomena and rogue wave solutions for an extended KP hierarchy-type equation by neural network-based method, *Ain Shams Eng. J.*, **16** (2025), 103657. https://doi.org/10.1016/j.asej.2025.103657

11. M. A. El-Shorbagy, S. Akram, M. ur Rahman, Propagation of solitary wave solutions to (4+1)-dimensional Davey-Stewartson-Kadomtsev-Petviashvili equation arise in mathematical physics and stability analysis, *Part. Differ. Eq. Appl. Math.*, **10** (2024), 100669. https://doi.org/10.1016/j.padiff.2024.100669
12. M. ur Rahman, S. Akram, M. Asif, Exploration of nonclassical symmetries and exact solutions to the (4+1)-dimensional Boiti-Leon-Manna-Pempinelli equation, *Sci. Rep.*, **15** (2025), 34652. https://doi.org/10.1038/s41598-025-20839-4
13. A. M. Mubaraki, R. I. Nuruddeen, K. K. Ali, J. F. Gómez-Aguilar, Additional solitonic and other analytical solutions for the higher-order Boussinesq-Burgers equation, *Opt. Quant. Electron.*, **56** (2024), 165. https://doi.org/10.1007/s11082-023-05744-2
14. R. F. Zhang, M. C. Li, H. M. Yin, Rogue wave solutions and the bright and dark solitons of the (3+1)-dimensional Jimbo-Miwa equation, *Nonlinear Dyn.*, **103** (2021), 1071–1079. https://doi.org/10.1007/s11071-020-06112-5
15. R. F. Zhang, S. Bilige, T. Chaolu, Fractal solitons, arbitrary function solutions, exact periodic wave and breathers for a nonlinear partial differential equation by using bilinear neural network method, *J. Syst. Sci. Complex.*, **34** (2021), 122–139. https://doi.org/10.1007/s11424-020-9392-5
16. R. F. Zhang, M. C. Li, M. Albishari, F. C. Zheng, Z. Z. Lan, Generalized lump solutions, classical lump solutions and rogue waves of the (2+1)-dimensional Caudrey-Dodd-Gibbon-Kotera-Sawada-like equation, *Appl. Math. Comput.*, **403** (2021), 126201. https://doi.org/10.1016/j.amc.2021.126201
17. R. F. Zhang, M. C. Li, A. Cherraf, S. R. Vadyala, The interference wave and the bright and dark soliton for two integro-differential equation by using BNNM, *Nonlinear Dyn.*, **111** (2023), 8637–8646. https://doi.org/10.1007/s11071-023-08257-5
18. R. F. Zhang, M. C. Li, J. Y. Gan, Q. Li, Z. Z. Lan, Novel trial functions and rogue waves of generalized breaking soliton equation via bilinear neural network method, *Chaos Soliton. Fract.*, **154** (2022), 111692. https://doi.org/10.1016/j.chaos.2021.111692
19. R. F. Zhang, S. Bilige, Bilinear neural network method to obtain the exact analytical solutions of nonlinear partial differential equations and its application to p-gBKP equation, *Nonlinear Dyn.*, **95** (2019), 3041–3048. https://doi.org/10.1007/s11071-018-04739-z
20. R. F. Zhang, S. Bilige, J. G. Liu, M. Li, Bright-dark solitons and interaction phenomenon for p-gBKP equation by using bilinear neural network method, *Phys. Scr.*, **96** (2021), 025224. https://doi.org/10.1088/1402-4896/abd3c3
21. Y. Liu, Z. Ma, R. Lei, Lump solution, interaction solution, and interference wave for the (3+1)-dimensional BKP-Boussinesq equation as well as analysis of BNNM model degradation, *Nonlinear Dyn.*, **112** (2024), 2837–2849. https://doi.org/10.1007/s11071-023-09169-0
22. N. M. Tuan, P. Meesad, A bilinear neural network method for solving a generalized fractional (2+1)-dimensional Konopelchenko-Dubrovsky-Kaup-Kupershmidt equation, *Int. J. Theor. Phys.*, **64** (2025), 17. https://doi.org/10.1007/s10773-024-05855-w
23. Z. Ma, Y. Liu, Y. Wang, The exact analytical solutions of the (2+1)-dimensional extended Korteweg-de Vries equation using bilinear neural network method and bilinear residual network method, *Mod. Phys. Lett. B*, **39** (2025), 2550045. https://doi.org/10.1142/S0217984925500459

24. Z. Zhao, B. Ren, Periodic solutions, breather, lump and interaction solutions of a generalized (2+1)-dimensional Hirota bilinear equation via the bilinear neural network method, *Commun. Theor. Phys.*, **77** (2024), 035001. https://doi.org/10.1088/1572-9494/ad8740

25. B. G. Konopelchenko, V. G. Dubrovsky, Some new integrable nonlinear evolution equations in 2+1 dimensions, *Phys. Lett. A*, **102** (1984), 15–17. https://doi.org/10.1016/0375-9601(84)90442-0

26. W. Ma, Generalized bilinear differential equations, *Stud. Nonlinear Sci.*, **2** (2011), 140–144.

27. L. L. Huang, Y. Chen, Lump solutions and interaction phenomenon for (2+1)-dimensional Sawada-Kotera equation, *Commun. Theor. Phys.*, **67** (2017), 473. https://doi.org/10.1088/0253-6102/67/5/473

28. J. Li, Q. Chen, B. Li, Resonance Y-type soliton solutions and some new types of hybrid solutions in the (2+1)-dimensional Sawada-Kotera equation, *Commun. Theor. Phys.*, **73** (2021), 045006. https://doi.org/10.1088/1572-9494/abe366

29. H. Q. Zhang, W. X. Ma, Lump solutions to the (2+1)-dimensional Sawada-Kotera equation, *Nonlinear Dyn.*, **87** (2017), 2305–2310. https://doi.org/10.1007/s11071-016-3190-6

30. L. Q. Li, Y. T. Gao, L. Hu, T. T. Jia, C. C. Ding, Y. J. Feng, Bilinear form, soliton, breather, lump and hybrid solutions for a (2+1)-dimensional Sawada-Kotera equation, *Nonlinear Dyn.*, **100** (2020), 2729–2738. https://doi.org/10.1007/s11071-020-05600-y

31. C. K. Kuo, Resonant multi-soliton solutions to the (2+1)-dimensional Sawada-Kotera equations via the simplified form of the linear superposition principle, *Phys. Scr.*, **94** (2019), 085218. https://doi.org/10.1088/1402-4896/ab11f5

32. H. An, D. Feng, H. Zhu, General M-lump, high-order breather and localized interaction solutions to the 2+1-dimensional Sawada-Kotera equation, *Nonlinear Dyn.*, **98** (2019), 1275–1286. https://doi.org/10.1007/s11071-019-05261-6

33. Z. Qi, Q. Chen, M. Wang, B. Li, New mixed solutions generated by velocity resonance in the (2+1)-dimensional Sawada-Kotera equation, *Nonlinear Dyn.*, **108** (2022), 1617–1626. https://doi.org/10.1007/s11071-022-07248-2

AIMS Press